44th AIAA Aerospace Sciences Meeting and Exhibit
9-12 January 2006, Reno, Nevada

AIAA 2006-1356

Blast Wave Energy Conversion Process in a Line-Focusing Laser Supported Detonation Waves

Masato Ushio*, Koichi Kawamura*, Kimiya Komurasaki†,
The University of Tokyo, Kashiwa-shi, Chiba 277-8562, JAPAN

Hiroshi Katsurayama‡, and Yoshihiro Arakawa§
The University of Tokyo, Bunkyo-ku, Tokyo,113-8656, JAPAN

Laser Supported Detonation (LSD) waves were driven by a line-focusing laser beam in two-dimensional and quasi-one-dimensional space, and visualized by the shadowgraph method. The blast eave energy and LSD termination condition were estimated from the wave propagation characteristics. As a result, fractional laser absorption during the LSD regime for 2D and quasi-1D cases was 68% and 81%, respectively, which was lower than that of three-dimensional LSD wave driven by a point-focusing beam (typically 90%). However, the blast wave energy efficiency was found proportional to the fractional absorption. Besides, the LSD threshold intensity was apparently lowered in the quasi-1D case due to the momentum confinement effect.

Nomenclature

E_i	=	irradiated laser pulse energy
E_{bw}	=	blast wave energy
M_s	=	shock wave propagation Mach number
r_s	=	radius of cylindrical blast wave
S_{LSD}	=	laser supported detonation (LSD) termination threshold laser intensity
S_{bw}	=	area driven by blast wave
α	=	apex angle of the blast wave expansion area
γ	=	specific heat
η_{bw}	=	fraction of blast wave energy to irradiated laser pulse energy
η_{LSD}	=	fraction of cumulative irradiated laser energy while LSD to irradiated laser pulse energy
ρ_a	=	ambient air density
ξ_0	=	blast wave parameter

I. Introduction

Air-breathing Repetitively Pulsed (RP) laser propulsion is a candidate for a low-cost launcher. Thrust impulse is generated through the following processes. A breakdown of the atmospheric air occurs by focusing an intense laser pulse. Plasma propagates along the laser light channel absorbing the laser energy. The absorption occurs in two regimes: One is a Laser Supported Detonation (LSD) regime at the intensity higher than the order of 10^7 W/cm^2, and the other is a Laser Supported Combustion (LSC) regime at the intensity lower than 10^6 W/cm^2. In the LSD regime, laser energy is absorbed in the vicinity of a shock wave, which is called a LSD wave. In the LSC regime, the shock front and the plasma front have been separated, and the laser energy is absorbed by the plasma left

* Graduate student, Department of Advanced Energy, The University of Tokyo, 5-1-5, Kashiwanoha, Kashiwa-shi, Chiba, 277-8561, JAPAN
† Associate Professor, Department of Advanced Energy, The University of Tokyo, 5-1-5, Kashiwanoha, Kashiwa-shi, Chiba, 277-8561, JAPAN, Member AIAA.
‡ Graduate student, Department of Aeronautics and Astronautics, The University of Tokyo, 7-3-1 Hongo, Bunkyo-ku, Tokyo, 113-8658, JAPAN, Member AIAA
§ Professor, Department of Aeronautics and Astronautics, The University of Tokyo, 7-3-1 Hongo, Bunkyo-ku, Tokyo, 113-8658, JAPAN, Member AIAA.

behind the shock front. A blast wave, which imparts thrust to a nozzle wall, is mainly driven in the LSD regime. Hence the energy conversion in the LSD regime is important to predict the thrust performance of RP laser propulsion.

Mori et al.[1, 2] characterized the blast wave driven by a point-focusing laser beam with various focusing f-number, total laser energy and ambient pressure using the shadowgraph method (Figs.1 and 2). They evaluated the laser intensity threshold S_{LSD} at LSD termination and the blast wave energy E_{bw} which is the source energy necessary to drive an equivalent blast wave in a calorically perfect gas. Fukuda et al.[3] investigated the electron density distribution in the LSC regime using the Mach-Zehnder interferometry (Fig.3).

In these experiments, blast waves were driven by a point-focusing laser beam. However, to realize really high power laser vehicles, a line-focusing technique would be inevitable. In line-focusing optics, laser intensity at the focal line is controllable, and there is a possibility of reduction in radiation and frozen flow losses because the peak intensity in the vicinity of focal line can be lowered comparing with the point-focusing case. The line-focusing technique has also been used in the Lightcraft.[5]

In this paper, LSD waves driven by a line-focusing laser beam were visualized using the shadowgraph method.

II. Experimental Set-Up

The experimental set-up in this study is composed of 2D LSD and quasi 1-D wave generating apparatus and, shadowgraph imaging apparatus. Figure 3 shows a schematic of the experimental apparatus.

A. Apparatus Generating 2-D and Quasi-1D LSD

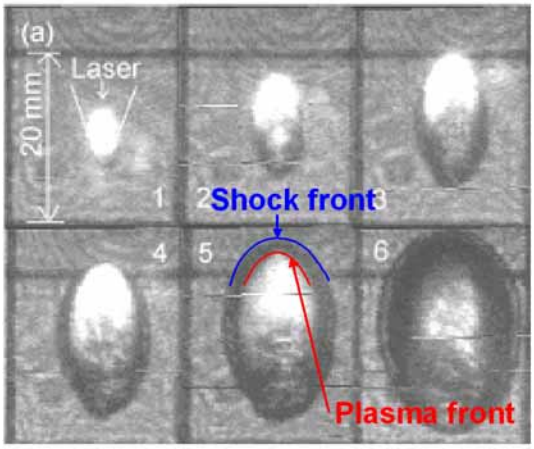

Figure 1. Shadowgraphs of laser-induced plasma expansion in the atmospheric air[1], t= (1) 0.25μs, (2) 1.0μs, (3) 2.0μs, (4) 3.0μs, (5) 4.0μs, (6) 5.0μs.

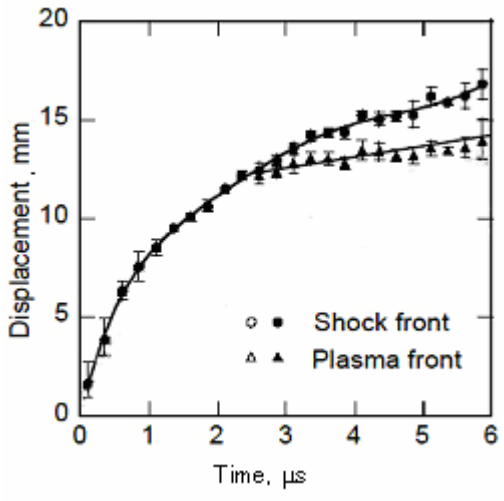

Figure 2. History of the shock front and plasma front displacements on the laser axis deduced from the shadowgraphs in the case of point-focusing laser beam.[1]

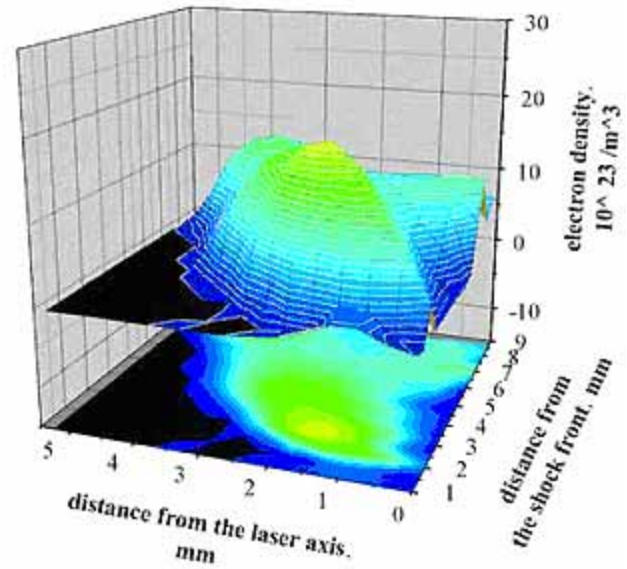

Figure 3. Electron density distribution on the laser axis in the LSC regime measured by the Mach-Zehnder interferometry.[3]

A 10 J Transversely Excited Atmospheric (TEA) CO2 pulse laser was used to generate LSD. The laser pulse shape is shown in Fig.4. The beam cross section is a square of 30mm×30mm. It was focused on an aluminum plate to initiate the breakdown in the atmospheric air. An off-axis line-focusing parabolic mirror was used to focus the laser beam. Its focal length was 48mm, and the ratio of focal length to beam width was 1.5. As shown in Fig.5 (a), two glass walls were attached perpendicularly to the aluminum plate to get rid of the edge effect. Besides, an aluminum wedge nozzle was used to realize quasi-1D LSD wave propagation by limiting the blast wave expansion in the direction of laser incidence as shown in Fig.5 (b). Apex angle of the nozzle was set slightly smaller that of the focusing laser channel.

B. Shadowgraph imaging apparatus

Figure 6 shows a schematic of the shadowgraph system. A He-Ne laser (633nm 12mW CW) was used as a light source. Pictures were taken by an Image-intensified Charged Couple Device (ICCD) camera (Oriental Instruments InstaSpec™ V ICCD detector, model 77193-5).

Optical emission from a gap switch of TEA CO2 pulse

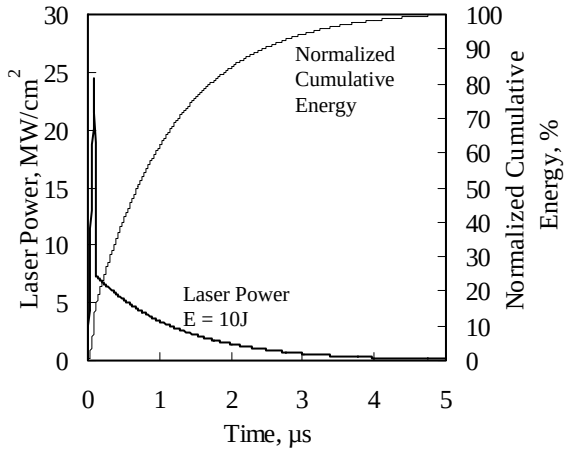

Figure 4. Laser pulse shape of the 10J TEA CO2 pulse laser.

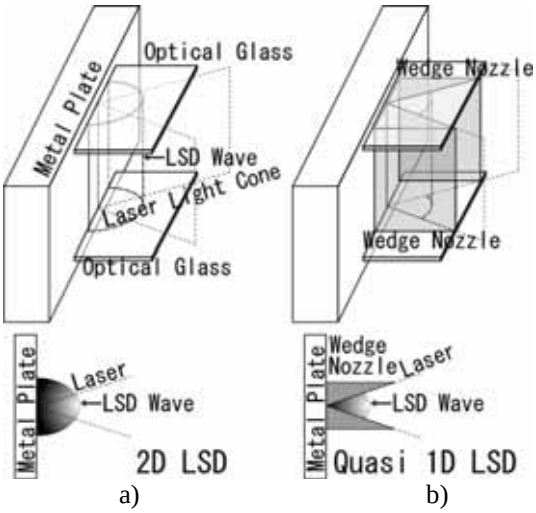

Figure 5. Schematic of the targets for a) 2D and b) quasi-1D LSD generation.

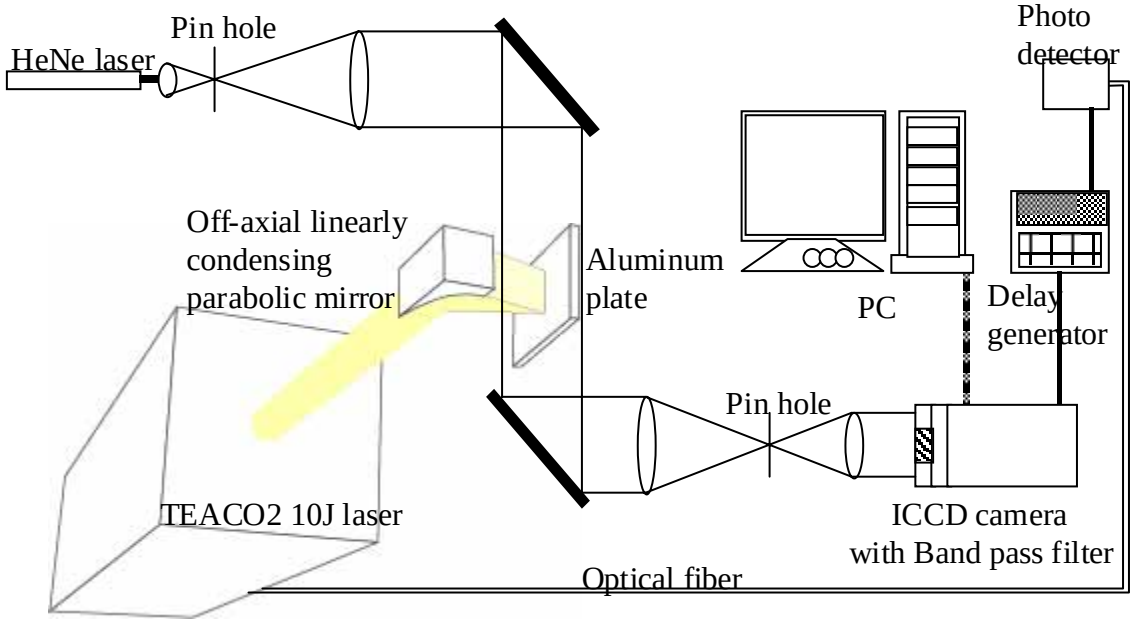

Figure 6. Schematic of the experimental apparatus.

laser was transmitted to the ICCD camera through a delay-circuit so as to trigger the camera with arbitrary delay. Emission from the plasma was reduced using a pinhole, and band-pass filters that transmit the wavelength of 633nm with FWHM of 1nm.

III. Results

Figures 7 and 8 show the shadowgraphs of a 2D and quasi-1D LSD waves respectively. In these figures, laser started to irradiate at t=0μs. Figure 9 shows temporal variation of the shock and plasma front displacements on the laser axis. As seen in the figure, the shock front and plasma front began to separate at 1.3μs for the 2D LSD and 1.8μs for the quasi-1D LSD.

The blast wave energy E_{bw} was deduced from the observed shock propagation characteristics using the self-similar equation.[5] According to the self-similar equation of a cylindrical blast wave,[6] time varying radius $r_s(t)$ initiated at t=0 is expressed as

$$r_s(t) = \xi_0 \left(\frac{E_{bw} / (\alpha / 2\pi)}{\rho_a} \right)^{\frac{1}{4}} t^{\frac{1}{2}} \tag{1}$$

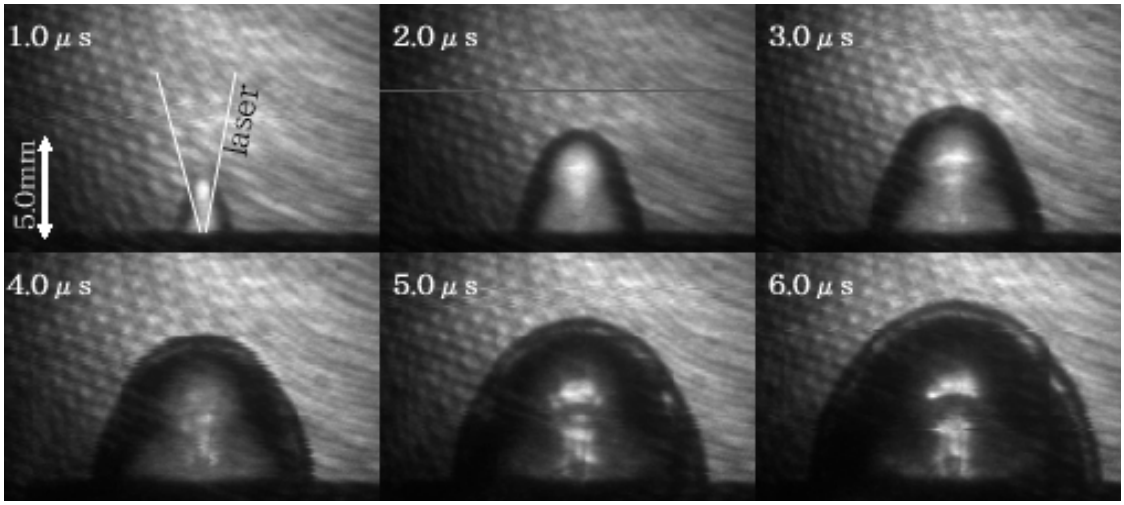

Figure 7. Shadowgraphs of the evolution of a 2D LSD wave. Laser started to irradiate at 0μs.

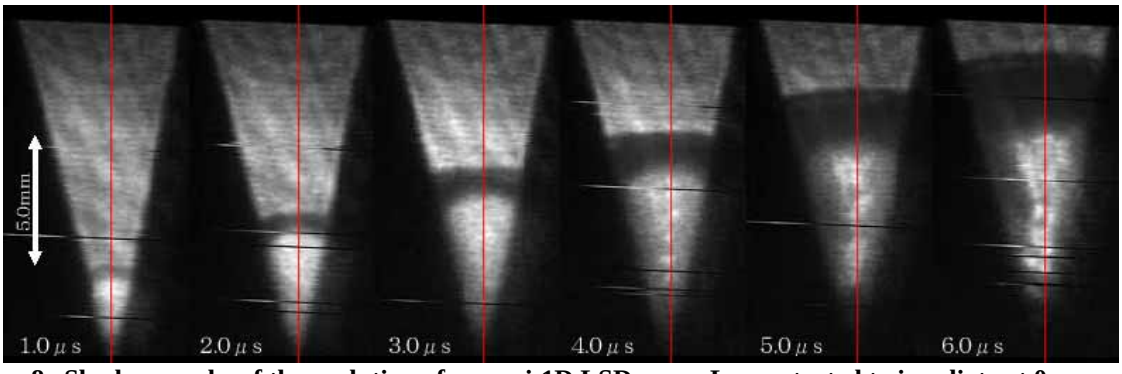

Figure 8. Shadowgraphs of the evolution of a quasi-1D LSD wave. Laser started to irradiate at 0μs.

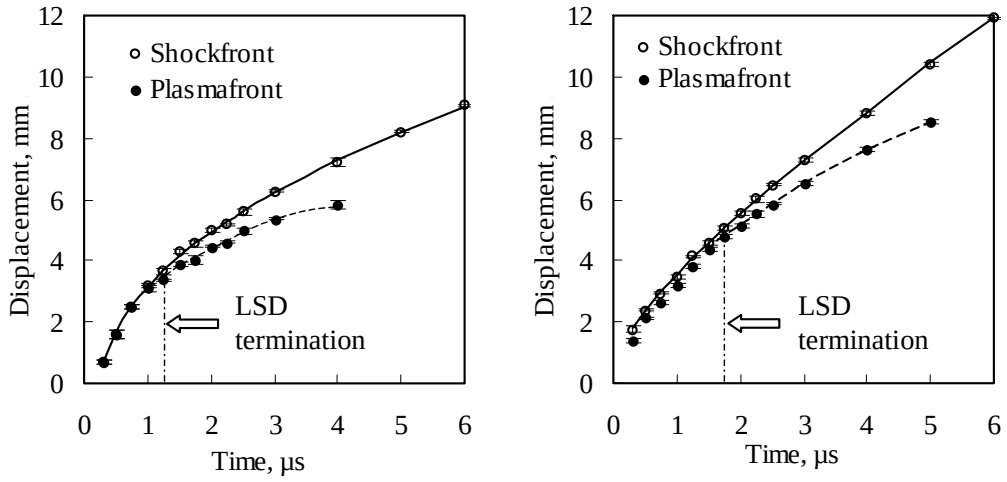

Figure 9. Displacements of the shock and plasma front of a) the 2D and b) the quasi-1D LSD.

where ξ_0 is a blast wave parameter which is a function of specific heat γ and its value is 1.00 for γ = 1.4. ρ_a is the ambient density (=1.28[kg/m3]) and α is the apex angle of the blast wave expansion area; $\alpha=\pi$ for 2D case, and 0.24 rad for quasi-1D case. Although the self-similar solution is inaccurate for intermediate shock strengths, it is still a good approximation for when M_s is at 2 - 3 according to the comparison with a perturbation solution for a cylindrical blast wave.[7] On the contrary, calorically perfect gas assumption (γ=const, then ξ_0=const) is valid approximately for M_s<4 in the 1atm air according to the comparison of the analysis of blast wave in perfect gas with that in real gas.[8]

Rewriting Eq. (1), the blast wave area S_{bw} is expressed as a linear function of time as,

$$S_{\mathrm{bw}} = \frac{\alpha}{2}\cdot r_s^2 = \frac{\alpha}{2}\xi_0^2\sqrt{\frac{2\pi E_{\mathrm{bw}}}{\alpha\rho_a}}\cdot(t-t_0) \equiv A(t-t_0) \tag{2}$$

where A is a proportional constant and t_0 is the experimental time-lag from an ideal point source expansion. This equation can be applied even to elliptical expansion cases as seen in Fig.7, using the Kompaneets approximation.[9] Thus the blast wave energy was calculated.

After the LSD has terminated, laser energy cannot drive the shock wave because LSC heating becomes almost adiabatic. Therefore, energy input to the blast wave is terminated when the LSD has terminated.

E_{bw} was calculated from the inclination of $S_{bw}(t)$ for M_s<5 as shown in Fig.10. The blast wave energy efficiency η_{bw} is defined as

$$\eta_{\mathrm{bw}} = E_{\mathrm{bw}} / E_i \tag{3}$$

where E_i is the irradiated laser energy.

In Table 1, deduced η_{bw} are listed along with the LSD termination conditions, such as the termination time t_{LSD}, laser intensity threshold S_{LSD} and Mach numbers M_{LSD}. In the 2D and the quasi-1D cases, LSD was terminated earlier than 3D cases because of lower laser intensity on the LSD wave, resulting in lower η_{bw}. However, S_{LSD} in the quasi-1D case was apparently lower than the other cases.

Table 1. η_{bw}, and LSD termination conditions.

Dimension of phenomena	2D	Quasi-1D	3D
Focal Length / Beam Diameter	1.5	2.0	2.2
η_{bw} [%]	33	37	44
t_{LSD} [μs]	1.2	1.8	2.5
S_{LSD} [MW/cm^2]	3.4	1.7	3.7
M_{LSD}	5.3	6.3	5.4

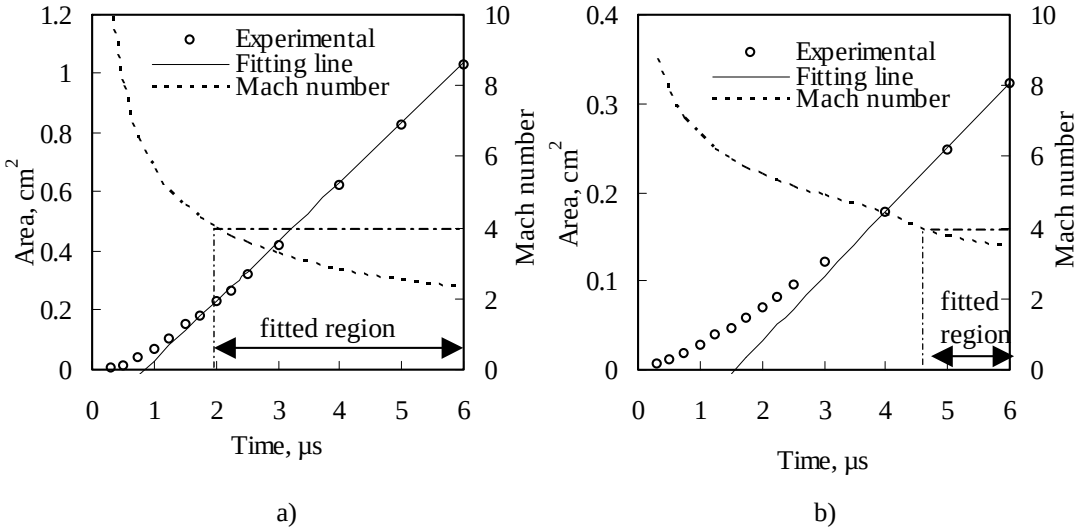

Figure 10. Temporal variation of the blast wave area $S_{bw}(t)$ and shock wave propagation Mach number M_s for a) the 2D and b) the quasi-1D LSD. $S_{bw}(t)$ was fitted by the self-similar solution within the region shown in the figure.

IV. Discussions

Fractional laser absorption η_{LSD} (=Cumulative energy until LSD termination / Total irradiated energy) and η_{bw} are listed in Table 2. As seen in the table, η_{bw} is proportional to η_{LSD} for all cases. Therefore, the decrease in η_{bw} can be attributed to that in η_{LSD}. This also indicates that reduction in radiation and frozen flow losses by decreasing the peak laser intensity in the vicinity of focal line was not appreciable in this range of energy.

Table 2. Fractional laser energy absorption while LSD η_{LSD}, and η_{bw}.

Dimension of phenomena	2D	Quasi 1D	3D
Focal Length / Beam Diameter	1.5	2.0	2.2
η_{bw} [%]	33	37	44
η_{LSD} [%]	68	81	90
η_{bw} /η_{LSD} [%]	49	47	49

However, S_{LSD} in the quasi-1D case was apparently lower than those in other cases as seen in Table 1. Therefore, there is a possibility to have high η_{LSD} in LSD confinement configuration by optimizing the matching of the laser pulse shape and variation of the laser cross section.

Measured quasi-1D LSD propagation was compared with the quasi-1D LSD simulation.[10] In the simulation, real gas effects are taken into account assuming thermo-chemical equilibrium at the LSD front represented as planer wave propagating along the laser light channel as schematically shown in Fig. 11. The Chapman-Jouguet detonation velocity is determined from the shock relations assuming 100% laser absorption in the LSD regime, which was assumed terminated when the laser intensity on the wave front becomes equal to the measured threshold intensity S_{LSD}.

Figure 12 shows the measured and computed shock front displacements. As seen in the figure, computed LSD propagated faster than measured one. This would be because of the absence of nonequilibrium effects and radiation loss: In nonequilibrium condition, electron temperature will be higher and heavy particle temperature lower than

equilibrium temperature. Radiation loss will also decrease the temperature. These effects will slow down the LSD propagation.

The measured quasi-1D LSD data will be useful to develop a reliable physical model of LSD phenomena.

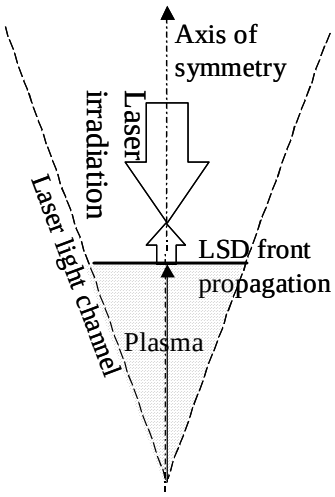

Figure 11. The model of quasi-1D LSD simulation.

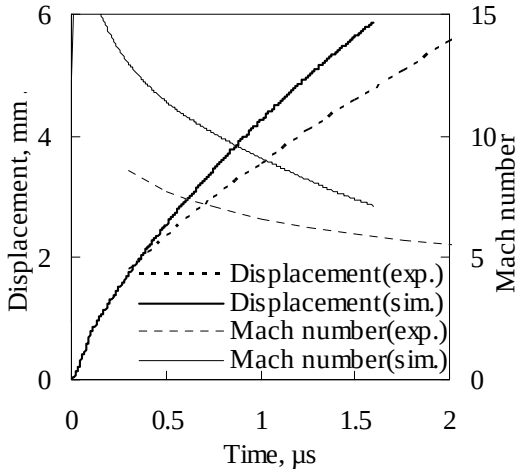

Figure 12. Displacements and propagation Mach number M_s of the quasi-1D LSD front in simulation and experiment. (exp. stands for experiment and sim. stands for simulation.)

V. Conclusions

In the line-focusing cases, LSD was terminated earlier than the point-focusing cases because of lower laser intensity on the LSD wave, resulting in lower fractional laser absorption.

The blast wave energy efficiency was proportional to the fractional laser absorption for all cases. This indicates that reduction in radiation and frozen flow losses by decreasing the peak laser intensity was not appreciable in this range of energy. By using higher power laser, this effect may be observed.

In the quasi-1D case, the LSD threshold laser intensity was apparently lower than those in other cases. Therefore, there is a possibility to have higher fractional laser absorption in LSD confined configuration by optimizing the matching of the laser pulse shape and variation of the laser cross section along the laser channel.

Computed LSD propagated faster than measured one because of the absence of nonequilibrium effects and radiation loss. The results of this experiment will be useful to validate the quasi-1D LSD simulation considering these effects.

References

[1]Mori, K., Komurasaki, K., and Arakawa, Y., "Influence of the Focusing f-Number on Heating Regime Transition in Laser Absorption Waves," *Journal of Applied Physics*, Vol.92, No.10, pp.5663~5667, 2002

[2]Mori, K., Komurasaki, K. and Arakawa, Y., "Energy Transfer from a Laser Pulse to a Blast Wave in Reduced-Pressure Air Atmospheres," *Journal of Applied Physics*, Vol. 95, No. 11, pp. 5979~5983, 2004

[3]Fukuda, A., Hirooka, Y., Mori, K., Komurasaki, K., and Arakawa, Y., "Electron Density Measurement of Laser Supported Detonation Waves," AIAA-2004-2565, *Plasmadynamics and Lasers Conference*, 35th, Portland, Oregon, June 28-1, 2004

[4]Myrabo, L. N., (Lightcraft Technologies, Inc., Bennington, VT) "World Record Flights of Beam-Riding Rocket Lightcraft - Demonstration of "Disruptive" Propulsion Technology," AIAA-2001-3798, AIAA/ASME/SAE/ASEE *Joint Propulsion Conference and Exhibit*, 37th, Salt Lake City, UT, July 8-11, 2001

[5]Sedov, L. I., *Similarity and Dimension Methods in Mechanics*, Academic Press, New York, 1959.

[6]Bach, G. G., Lee, J. H., "Higher-Order Perturbation Solutions for Blast Waves," *AIAA Journal*, Vol. 7, (1969), pp.742–744.

[7]Radulescu, M. I., Higgin, A. J., Murray, S. B., Lee, J. H. S., "An Experimental Investigation of the Direct Initiation of Cylindrical Detonations," *Journal of Fluid Mechanics*, Vol. 480, (2003), pp. 1–24.

[8]Gretler, W., "Blast Waves in Inhomogeneous Atmospheres Including Real Gas and Heat Transfer Effects," *Fluid Dynamics Research*, Vol. 14 (1994) pp.191-216

[9]Kompaneets, A. S., "A Point Explosion in an Inhomogeneous Atmosphere," *Soviet Physics Doklady*, 5(1960), pp.46-48

[10]Katsurayama, H., Komurasaki, K., Arakawa, Y., "A 1-D Model of Laser Supported Detonation Wave in Laser-Plasma Energy Conversion," *Journal of IAPS, Applied Plasma Science* Vol. 12, (2004), pp.17-22 (In Japanese).